VIP Hydride Complexes

DOI: 10.1002/anie.201301706

Identifying Intermediates of Sequential Electron and Hydrogen Loss from a Dicarbonylcobalt Hydride Complex**

*Michael J. Krafft, Martina Bubrin, Alexa Paretzki, Falk Lissner, Jan Fiedler, Stanislav Záliš, and Wolfgang Kaim**

Coordination compounds of cobalt have recently received special attention in the context of hydrogen production ("splitting water with cobalt")[1] and conversion.[1–9] Within these studies the mechanistic sequence of electron and proton or hydrogen transfer has frequently been discussed. Although cobalt carbonyl hydrides, especially $[Co(CO)_4H]$ have been the subject of many studies since their development by Hieber and co-workers in the 1930s[10] and since their use in hydroformylation processes, the hydrogen-producing reactions were mainly reported with non-organometallic cobalt complexes, involving ligands such as oligodentate imines, glyoximes, phosphanes, and macrocycles.[1–8]

Herein we describe the synthesis and characterization of the first dicarbonylhydridocobalt complex $[Co(CO)_2(dippf)H] = [(\mathbf{1})H]$ with a 1,1′-diphosphinoferrocene ligand (dippf = 1,1′-bis(diisopropylphosphino)ferrocene) and its chemical and (spectro)electrochemical oxidation via $[(\mathbf{1})H]^+$ to the structurally characterized product $[Co(CO)_2(dippf)]^+ = [(\mathbf{1})]^+$, which has formally lost a hydrogen atom and can be reduced to a Co^0 species $[(\mathbf{1})]$ (Scheme 1). In contrast to the above-mentioned complexes,[1–8] in our series the presence of CO ligands makes it possible to monitor several intermediates by IR spectroelectrochemistry.[11]

The family of 1,1′-bis(diorganophosphino)ferrocene ligands has been widely used in catalysis and for functional molecular materials;[12] these ligands can also be considered as redox noninnocent[13] due to the reversible oxidation of the ferrocene framework.[14] For instance, it was shown that the assignment of the oxidation site in ambivalent $[Fe^{II}Ru^{II}]$ heterobimetallic complexes involving 1,1′-bis(diorganophosphino)ferrocene ligands is not trivial.[14b]

Reaction of $[Co(CO)_4H]$ with dippf leads to compound $[(\mathbf{1})H]$.[15a] In addition to the ^1H and ^{31}P NMR spectroscopy the crystal structure analysis[15b] (Figure 1 A, Table 1) confirms the configuration with one metal–hydride bond (at a disordered position) pointing toward the inside—probably a result of the steric crowding from the P*i*Pr$_2$ groups at the outside. Both hydride positions (at half occupancy) were thus found crystallographically as capping the approximately tetrahedral CuP_2C_2 coordination core. DFT calculations confirm the experimental structure as a stable arrangement (Table 1, see also Figure S1 in the Supporting Information).

Cyclic voltammetry at ambient temperature (Figure 2 A) and at −50 °C in CH_2Cl_2 (Figure S2) showed an oxidation of

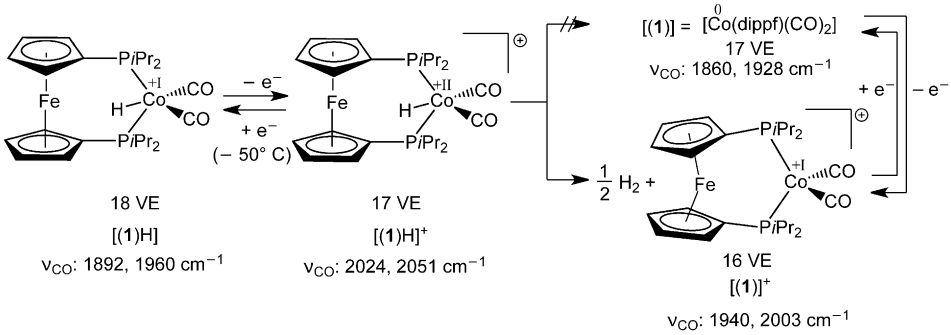

Scheme 1. Reaction mechanism derived in this study.

the 18 valence electron (VE) precursor $[(\mathbf{1})H]$ to the 17 VE species $[(\mathbf{1})H]^+$, leading to high-energy shifted ν_{CO} stretching bands in OTTLE spectroelectrochemistry[16] experiments (see Figure 3 A). Unfortunately, the intense CO stretching bands tend to obscure the weaker ν_{CoH} absorptions at around 2000 cm^{-1} which are calculated to shift only by a few wavenumbers (see Tables 2 and S3) in spite of the probably decreased M–H bond strength.[6,17] DFT calculations of the structure and of the CO and Co–H stretching frequencies of $[(\mathbf{1})H]$ and of $[(\mathbf{1})H]^+$ are summarized in Tables 1 and 2 and in Figure S1; simulated IR spectra are shown in Figure S5 in the Supporting Information.

The absorption maximum of $[Co^{II}\text{-}H]^+$ lies at rather low energy (875 nm, see Figure S10) and the corresponding transition can be attributed to an MC/MLCT (metal cen-

[*] Dipl.-Chem. M. J. Krafft, Dipl.-Chem. M. Bubrin, Dipl.-Chem. A. Paretzki, Dr. F. Lissner, Prof. Dr. W. Kaim
Institut für Anorganische Chemie, Universität Stuttgart
Pfaffenwaldring 55, 70550 Stuttgart (Germany)
E-mail: kaim@iac.uni-stuttgart.de
Dr. J. Fiedler, Dr. S. Záliš
J. Heyrovský Institute of Physical Chemistry, v.v.i.
Academy of Sciences of the Czech Republic
Dolejškova 3, CZ-18223 Prague (Czech Republic)

[**] We thank the State of Baden-Württemberg, the Deutsche Forschungsgemeinschaft, and the COST program (CM1202) of the EU for financial support. We thank M. Eng. P. Eversfield, Institut für Technische Chemie, Universität Stuttgart, for H_2 gas analysis. S.Z. thanks the Ministry of Education of the Czech Republic (grant LD11086) for support.

Supporting information for this article is available on the WWW under http://dx.doi.org/10.1002/anie.201301706.

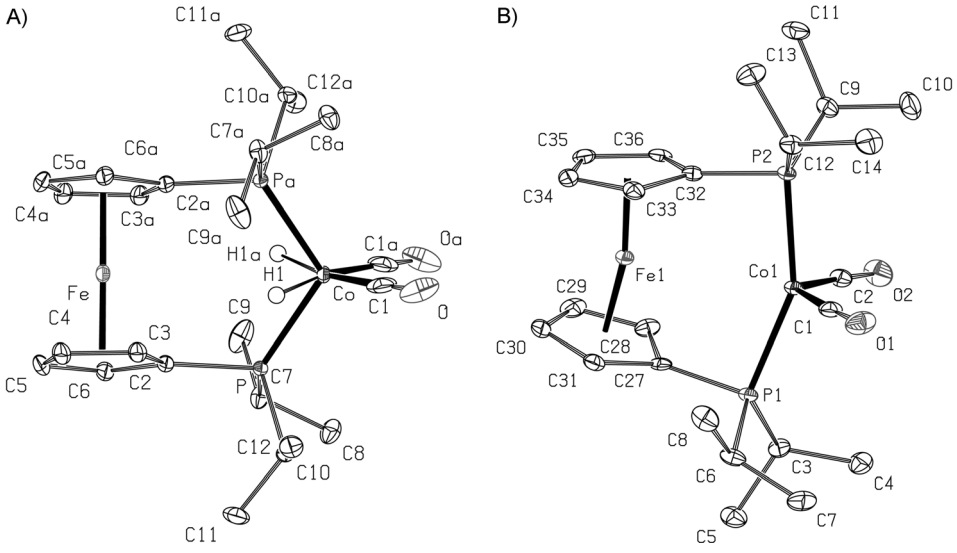

Figure 1. A) Molecular structure of [(**1**)H] in the crystal (disorder of one hydride at positions H1 and H1a, both positions shown with half occupancy) and B) molecular structure of the cation in [(**1**)](PF$_6$)·1 THF.

Table 1: Comparison of selected experimental and DFT-calculated structure parameters (distances in Å, angles in °).

	[(**1**)H]		[(**1**)H]$^+$	[(**1**)]$^+$	
	expt.	calc.[a]	calc.[a]	expt.	calc.[b]
Bond					
Co–C	1.736(2)	1.729	1.779	1.741(3)	1.726
Co–C	1.736(2)	1.730	1.804	1.774(3)	1.747
Co–P	2.1767(6)	2.169	2.257	2.1824(8)	2.171
Co–P	2.1767(6)	2.177	2.262	2.1665(9)	2.170
Co···Fe	4.1377(5)	4.117	3.837	3.2828(8)	3.357
Co–H	[1.58(4)]	1.478	1.473	–	–
Angle					
P-Co-P	114.08(2)	113.9	127.0	153.85(3)	150.2
C-Co-C	101.6(2)	97.6	96.5	127.3(1)	135.3
P-Co-C	105.32(7)	101.8	103.1	93.49(9)	94.0
		102.8	104.0	97.22(9)	95.2
	115.04(7)	116.4	110.4	95.81(9)	96.4
		119.6	110.5	96.44(9)	96.8
Cp–Cp[c]	1.3	0.0	0.5	16.0	9.5

[a] Averaged values. [b] ^{1}A state. [c] Dihedral angles.

tered/metal-to-ligand charge transfer) process according to TD-DFT calculations. After the loss of hydrogen the absorption maximum shifts to higher energies at 480 nm (Table 2; Figure S6 in the Supporting Information).

The oxidation of [(**1**)H] can occur either at the ferrocene or at the dicarbonylhydridocobalt(I) center. Earlier studies of ruthenium and osmium complexes of 1,1′-diphosphinoferrocene ligands have demonstrated a related ambivalence, depending on the other ligands and substituents.[14] The experimental and computational results for [(**1**)H]$^+$ and for the [(**1**)]$^+$/[(**1**)] couple (cf. below) show that the potentially redox-active ferrocene moiety is not directly involved in electron transfer, that is, displaying "innocent" behavior;[13] all redox processes occur at the cobalt site, involving 17 VE intermediates. Figure 2 A illustrates that a second (irreversible) oxidation of [(**1**)H] follows the first one at about 0.5 V more positive potential, presumably involving the ferrocene group at a typical value of +0.1 V versus [FeCp$_2$]$^{+/0}$.

At room temperature the cyclic voltammetric and IR-spectroelectrochemical monitoring of the oxidation shows the appearance of a follow-up product of the electron transfer [(**1**)H]→[(**1**)H]$^+$ in the form of the hydride-free [(**1**)]$^+$ (Figures 2 A and 3 B). This ion could also be obtained synthetically[15a] as the sensitive material [(**1**)](PF$_6$)·1 THF by reacting [(**1**)H] with ferrocenium hexafluorophosphate accompanied by the evolution of GC-detected H$_2$ gas (see the Supporting Information). The ^{1}H NMR data and the crystal structure analysis[15b] confirm the absence of a hydride ligand and indicate a highly stretched chelate configuration (Figure 1 B, Table 1). The remarkable structure of the 16 VE cobalt(I) compound [(**1**)]$^+$ with its obtuse angles of 153.85(3)° (P-Co-P) and

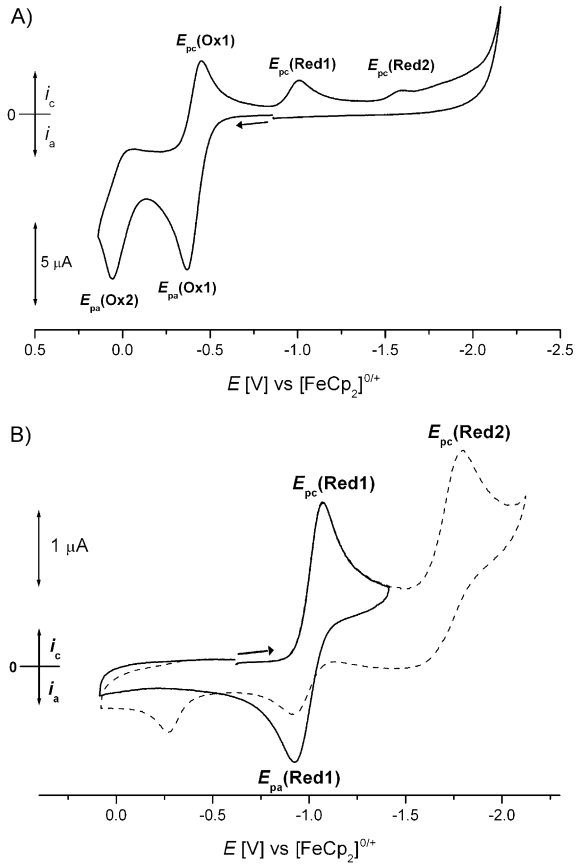

Figure 2. Cyclic voltammograms of [(**1**)H] (A) and of [(**1**)](PF$_6$) (B) at a scan rate of 100 mV s^{-1} in CH$_2$Cl$_2$/0.1 M Bu$_4$NPF$_6$.

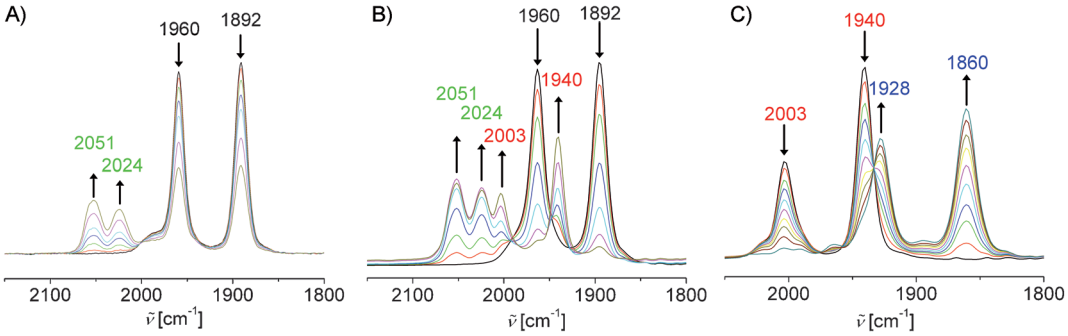

Figure 3. IR spectroelectrochemistry of the transitions [(**1**)H]/[(**1**)H]$^+$ at 213 K (A) and of the conversions [(**1**)H]/[(**1**)H]$^+$ (green)/[(**1**)]$^+$ (red) at 293 K (B) and of the transition [(**1**)]$^+$/[(**1**)] at 293 K (C), all in CH_2Cl_2/0.1 M Bu_4NPF_6.

Table 2: Electrochemical and spectroscopic data of complexes.[a]

	[(**1**)H]	[(**1**)H]$^+$	[(**1**)]$^+$	[(**1**)]$^-$
E [V][b]	$E_{1/2}$(ox1): −0.43		$E_{1/2}$(red1): −0.99	
E [V][b]	E_{pa}(ox2): +0.06		E_{pc}(red2): −1.79	
ν_{CO} [cm^{-1}][c]	1892 (1897)	2024 (2038)	1940 (1938)	1860 (1875)
ν_{CO} [cm^{-1}][c]	1960 (1959)	2051 (2057)	2003 (2002)	1928 (1935)
ν_{CoH} [cm^{-1}][c]	2000 br[d] (2006)	1980 br[d] (1993)		
λ_{max} [nm][e]	420 sh	875, 450 sh	480	380 sh

[a] (**1**) = [Co(dippf)(CO)$_2$]. [b] Potentials in V versus ferrocene/ferrocenium from cyclic voltammetry at a scan rate of 100 mV s^{-1} in CH_2Cl_2/0.1 M Bu_4NPF_6. [c] Experimental values from spectroelectrochemistry (OTTLE cell) in CH_2Cl_2/0.1 M Bu_4NPF_6, DFT calculated values in parentheses (scaling factor 0.946). [d] Obscured by CO stretching band. [e] Absorption maxima from spectroelectrochemistry (OTTLE cell) in CH_2Cl_2/0.1 M Bu_4NPF_6.

127.3(1)° (C-Co-C) could be reproduced by DFT calculations, illustrating the approach to a square-planar configuration. In spite of the significant shortening of the Fe–Co distance by 0.9 Å there is no metal–metal bonding[18] according to the DFT calculations.

Cyclic voltammetry, EPR, and IR spectroelectrochemistry show that the 16 VE species [(**1**)]$^+$ is reversibly reduced to a 17 VE cobalt(0) compound [(**1**)] (Figures 2 B, 3 C, and S7, as well as Table 2). The paramagnetic intermediate forms containing [Co^{II}-H]$^+$ ([(**1**)H]$^+$) and Co^0 ([(**1**)]) exhibit broad, complex EPR spectra in frozen solution (Figure S8) which are compatible with cobalt-centered spin as confirmed by DFT spin density calculations (Figure S9).

The carbonyl stretching frequencies of the four heterobimetallic compounds isolated or generated reflect the configuration at cobalt: Oxidation of the Co^I-H species [(**1**)H] produces a large high-energy shift of ν_{CO} in the [Co^{II}-H]$^+$ intermediate (Figure 3 A) which is somewhat attenuated on loss of hydrogen to give the isolated [Co^I]$^+$ form [(**1**)]$^+$ (Figure 3 B). Reduction of the latter to the neutral Co^0 species [(**1**)] results in a sizeable low-energy shift (Figure 3 C, Table 2).

The oxidation state changes [Co^I-H] (18 VE)→[Co^{II}-H]$^+$ (17 VE)→[Co^I]$^+$ (16 VE)→[Co^0] (17 VE) evidenced here for a dicarbonyldiphosphine ligated series [(**1**)H]⇌[(**1**)H]$^+$→[(**1**)]$^+$⇌[(**1**)] correspond to the mechanistic model [Co^{III}-H]→[Co^{II}]→[Co^I]$^-$ proposed for the monometal variant of cobalt-catalyzed H_2 generation.[4,19] The lower oxidation states in the present case result from the presence of CO and phosphines as acceptor ligands.

Summarizing, the complex [(**1**)H] is oxidized at the cobalt site to yield a spectroelectrochemically detected cationic intermediate [(**1**)H]$^+$ which converts homolytically to a hydride-free product [(**1**)]$^+$, isolated and structurally characterized as the hexafluorophosphate. In contrast to [(**1**)H] (P-Co-P 114.08(2)°, $d_{Fe\text{-}Co}$ 4.1377(5) Å)), the cation [(**1**)]$^+$ exhibits an obtuse P-Co-P bite angle of 153.85(3)° and a relatively short Fe–Co distance of 3.2828(8) Å, reflecting considerable structural flexibility of the potentially noninnocent dippf ligand. According to spectroelectrochemistry the reversible reduction of [(**1**)]$^+$ to the Co^0 species [(**1**)] takes place at the cobalt center. The sequence [(**1**)H]→[(**1**)H]$^+$→[(**1**)]$^+$ represents a unique spectroscopically proven example of the homolytic splitting of a Co–H bond at room temperature.

Received: February 27, 2013
Published online: May 10, 2013

Keywords: cobalt · electron transfer · ferrocene · hydride complexes · spectroelectrochemistry

[1] V. Artero, M. Chavarot-Kerlidou, M. Fontecave, *Angew. Chem.* **2011**, *123*, 7376; *Angew. Chem. Int. Ed.* **2011**, *50*, 7238.
[2] a) F. Lakadamyali, M. Kato, N. M. Muresan, E. Reisner, *Angew. Chem.* **2012**, *124*, 9515; *Angew. Chem. Int. Ed.* **2012**, *51*, 9381; b) W. M. Singh, T. Baine, S. Kudo, S. Tian, X. A. N. Ma, H. Zhou, N. J. DeYonker, T. C. Pham, J. C. Bollinger, D. L. Baker, B. Yan, C. E. Webster, X. Zhao, *Angew. Chem.* **2012**, *124*, 6043; *Angew. Chem. Int. Ed.* **2012**, *51*, 5941.
[3] a) M. Guttentag, A. Rodenberg, C. Bachmann, A. Senn, P. Hamm, R. Alberto, *Dalton Trans.* **2013**, *42*, 334; b) E. S. Andreiadis, P.-A. Jacques, P. D. Tran, A. Leyris, M. Chavarot-Kerlidou, B. Jousselme, M. Matheron, J. Pécaut, S. Palacin, M. Fontecave, V. Artero, *Nat. Chem.* **2012**, *5*, 48.
[4] a) S. C. Marinescu, J. R. Winkler, H. B. Gray, *Proc. Natl. Acad. Sci. USA* **2012**, *109*, 15127; b) C. N. Valdez, J. L. Dempsey, B. S.

Brunschwig, J. R. Winkler, H. B. Gray, *Proc. Natl. Acad. Sci. USA* **2012**, *109*, 15589; c) J. L. Dempsey, B. S. Brunschwig, J. R. Winkler, H. B. Gray, *Acc. Chem. Res.* **2009**, *42*, 1995; d) S. Fukuzumi, Y. Yamada, T. Suenobu, K. Ohkubo, H. Kotani, *Energy Environ. Sci.* **2011**, *4*, 2754.

[5] a) W. R. McNamara, Z. Han, P. J. Alperin, W. W. Brennessel, P. L. Holland, R. Eisenberg, *J. Am. Chem. Soc.* **2011**, *133*, 15368; b) W. R. McNamara, Z. J. Han, C.-J. Yin, W. W. Brennessel, P. L. Holland, R. Eisenberg, *Proc. Natl. Acad. Sci. USA* **2012**, *109*, 15594.

[6] a) G. M. Jacobsen, J. Y. Yang, B. Twamley, A. D. Wilson, R. M. Bullock, M. R. DuBois, D. L. DuBois, *Energy Environ. Sci.* **2008**, *1*, 167; b) E. S. Wiedner, J. Y. Yang, W. G. Dougherty, W. S. Kassel, R. M. Bullock, M. R. Dubois, D. L. Dubois, *Organometallics* **2010**, *29*, 5390; c) S. Y. Reece, J. A. Hamel, K. Sung, T. D. Jarvi, A. J. Esswein, J. J. H. Pijpers, D. G. Nocera, *Science* **2011**, *334*, 645; d) R. Ciancanelli, B. C. Noll, D. L. DuBois, M. R. DuBois, *J. Am. Chem. Soc.* **2002**, *124*, 2984.

[7] S. Losse, J. G. Vos, S. Rau, *Coord. Chem. Rev.* **2010**, *254*, 2492.

[8] X. Hu, B. S. Brunschwig, J. C. Peters, *J. Am. Chem. Soc.* **2007**, *129*, 8988.

[9] B. de Bruin, W. I. Dzik, S. Li, B. B. Wayland, *Chem. Eur. J.* **2009**, *15*, 4312.

[10] a) W. Hieber, F. Mühlbauer, E. A. Ehmann, *Chem. Ber.* **1932**, *65*, 1090; b) W. Hieber, H. Schulten, *Z. Anorg. Allg. Chem.* **1937**, *232*, 17.

[11] a) J. M. Smieja, C. P. Kubiak, *Inorg. Chem.* **2010**, *49*, 9283; b) *Spectroelectrochemistry* (Eds.: W. Kaim, A. Klein), Royal Society of Chemistry, Cambridge, **2008**; c) J. Fiedler, C. Nervi, D. Osella, M. J. Calhorda, S. S. M. C. Godinho, R. Merkel, H. Wadepohl, *J. Chem. Soc. Dalton Trans.* **2002**, 3705.

[12] D. J. Young, S. W. Chien, T. S. A. Hor, *Dalton Trans.* **2012**, *41*, 12655.

[13] a) W. Kaim, *Inorg. Chem.* **2011**, *50*, 9752; b) W. Kaim, *Eur. J. Inorg. Chem.* **2012**, 343.

[14] a) R. T. Hembre, J. S. McQueen, V. W. Day, *J. Am. Chem. Soc.* **1996**, *118*, 798; b) T. Sixt, M. Sieger, M. J. Krafft, D. Bubrin, J. Fiedler, W. Kaim, *Organometallics* **2010**, *29*, 5511; c) W. Kaim, T. Sixt, M. Weber, J. Fiedler, *J. Organomet. Chem.* **2001**, *637–639*, 167.

[15] a) For experimental details, see the Supporting Information. b) CCDC 924959 [(**1**)H] and CCDC 924960 [(**1**)](PF_6)·1 THF contain the supplementary crystallographic data for this paper. These data can be obtained free of charge from The Cambridge Crystallographic Data Centre via www.ccdc.cam.ac.uk/data_request/cif.

[16] M. Krejčik, M. Danek, F. Hartl, *J. Electroanal. Chem. Interfacial Electrochem.* **1991**, *317*, 179.

[17] a) M. Tilset, *J. Am. Chem. Soc.* **1992**, *114*, 2740; b) K. T. Smith, C. Rømming, M. Tilset, *J. Am. Chem. Soc.* **1993**, *115*, 8681; c) M. Tilset in *Comprehensive Organometallic Chemistry III*, *Vol. 1* (Eds.: R. H. Crabtree, D. M. P. Mingos), Elsevier, Amsterdam, **2007**, p. 279.

[18] a) K. Uehara, S. Hikichi, A. Inagaki, M. Akita, *Chem. Eur. J.* **2005**, *11*, 2788; b) M. Sato, H. Shigeta, M. Sekino, *J. Organomet. Chem.* **1993**, *458*, 199; c) M. Murata, S. Habe, S. Araki, K. Namiki, T. Yamada, N. Nakagawa, T. Nankawa, M. Nihei, J. Mizutani, M. Kurihara, H. Nishihara, *Inorg. Chem.* **2006**, *45*, 1108.

[19] a) J. T. Muckerman, E. Fujita, *Chem. Commun.* **2011**, *47*, 12456; b) B. H. Solis, S. Hammes-Schiffer, *J. Am. Chem. Soc.* **2011**, *133*, 19036.

